Global J. Environ. Sci. Manage. 9(3): 373-388, Summer 2023, Serial #35

Global Journal of Environmental Science and Management
(GJESM)

Homepage: https://www.gjesm.net/

Podcasts

ORIGINAL RESEARCH PAPER

Response surface methodology and adaptive neuro-fuzzy inference system for adsorption of reactive orange 16 by hydrochar

J. Oliver Paul Nayagam, K. Prasanna*

Department of Civil Engineering, SRM Institute of Science and Technology, Kattankulathur, Chengalpattu, Tamil Nadu, India

ARTICLE INFO

Article History:
Received 05 October 2022
Revised 7 November 2022
Accepted 10 December 2022

Keywords:
Adaptive neuro-fuzzy inference system
Hydrochar
Reactive orange-16 (RO 16)
Response surface methodology
Statistical error analysis

DOI: 10.22035/gjesm.2023.03.02

ABSTRACT

BACKGROUND AND OBJECTIVES: The prediction models, response surface methodology and adaptive neuro-fuzzy inference system are utilized in this study. This study delves into the removal efficiency of reactive orange 16 using hydrochar derived from the *Prosopis juliflora roots*. Hydrochar dose, pH, temperature, and initial reactive orange 16 concentration were studied in batch processes. The correlation coefficients for the batch processes were found to be 0.978 and 0.9999. The results denote that the adaptive neuro-fuzzy inference system predicted the reactive orange 16 removal efficiency more accurately than the response surface methodology model.
METHODS: *Prosopis juliflora roots* roots are converted into hydrochar to remove azo dye from textile waste water. *Prosopis juliflora roots* roots were collected from Ramanad District, Southern Tamil Nadu, India. The moisture content was lowered by drying for 24 hours at 103 degree celcius in an oven with hot air. This biomass was thermally destroyed at 300 degree celcius for 15 minutes without oxygen in an autoclave in a muffle furnace (heating rate: 5 degree celcius per minute). As soon as it reaches room temperature, the hydrochar residue of this biomass was used for adsorption investigations. The batch adsorption process was conducted for 6 hours in a 250 milliliter Erlenmeyer conical flask with a 100 milliliter working volume using an orbital shaker. The pH, dosage, concentration, and temperature are the four parameters chosen for this study to find the maximum removal efficiency of the dye from aqueous solutions. This study validated adaptive neuro-fuzzy inference system, an artificial neural network with a fuzzy inference system, using response surface methodology projected experimental run with Box–Behnken method.
FINDINGS: The adaptive neuro-fuzzy inference system model is created alongside the response surface methodology model to compare experimental outcomes. Experimental data was evaluated using a hybrid least square and gradient technique. Statistical and residual errors assessed experimental and mathematical model correctness. Experimental data matched the adaptive neuro-fuzzy inference system results. Statistical error analysis verified the model's accuracy and precision against experimental data.
CONCLUSION: Response surface methodology and adaptive neuro-fuzzy inference system optimized process conditions. At pH 2, 2 gram per litre hydrochar dosage, 35 degree celcius , and a reactive orange 16 starting concentration of 250 milligram per liter, removal effectiveness reached 86.1 percent. Adaptive neuro-fuzzy inference system predicted higher values than response surface methodology, with batch correlation coefficients of 0.9999 and 0.9997, respectively. Mathematical techniques can accurately estimate dye removal efficiency from aqueous solutions.

NUMBER OF REFERENCES	NUMBER OF FIGURES	NUMBER OF TABLES
44	10	5

*Corresponding Author:
Email: *prasannk@srmist.edu.in*
Phone: 091442 741 7819
ORCID: 0000-0001-7839-4503

Note: Discussion period for this manuscript open until October 1, 2023 on GJESM website at the "Show Article".

INTRODUCTION

Oxidation, sand filtration, electrochemical processes, membrane filtration, and precipitation are typical wastewater treatment methods (Gupta *et al.,* 2013). These technologies are ideal in removing suspended solids; other than membrane filtration, removing dissolved solids is difficult. However, membrane filtration is an expensive treatment option and this has led to the development of unique treatment approaches (Hussein *et al.,* 2018; Chinwetkitvanich *et al.,* 2000). Compared with other approaches, one of the best ways to remove pollutants from wastewater is by adsorption (Ghoneim *et al*., 2014) as the removal effectiveness of this process is exceptionally high. Adsorbents, such as clay, silicates, zeolite, lime, and activated carbon, are frequently employed. The widely held adsorbent for the removal of hazardous contaminants is activated carbon (Crini *et al*., 2006; Orshansky *et al*., 1997). However, the production expense of activated carbon is its most significant drawback. One of the most economical methods for removing contaminants is biosorption, which uses inactive or dead microorganisms to create the biosorbent (Kaur *et al*., 2017). Many researchers in the past have made biosorbent from waste compost, neem seeds, moringa seeds, and agricultural biomass (Nayagam and Prasanna, 2022). This biomass is used in the treatment of toxic metals and dyes in wastewater. Hydrochar is created from *Prosopis juliflora roots*, which has high carbon content and several functional groups that promote absorption (Tran *et al*., 2020). The potential of hydrochar depends on the thermal stability of the raw materials sourced in its production. Feedstock is often separated into two groups: wet and dry. Wet biomass is defined as having a moisture percentage of ≥30, whereas dry biomass is defined as having a moisture percentage ≤30. It is usually recommended to use biomass with very low moisture content as the feedstock for the production of hydrochar. This biomass's cellulose, hemicellulose, and lignin content will breakdown during thermal decomposition, and the more stable feedstock will disintegrate at higher temperatures, creating more pores on the surface and increasing the hydrochar's sorption capacity (Wu *et al*., 2008; Beesley *et al*., 2011). Optimizing contaminant removal parameters to reduce experimental trials is a growing issue (Yousif *et al*., 2018). For the purpose of displacing traditional experimental trials, many optimization technologies have been developed. The response surface methodology (RSM) predicts the output using two or more variables with a minimal number of experimental trials (Gopal *et al*., 2014; Deb *et al*., 2019; Ohale *et al*., 2017; Aravind *et al.,* 2015). The adaptive neuro-fuzzy inference system (ANFIS) is a promising optimization technique with the highest correlation coefficient.Complex nonlinear systems can perform better when ANFIS is used (Tejada *et al*., 2021). This study evaluated the use of *P. juliflora roots* in batch procedures for hydrochar synthesis and decolorization of reactive orange 16 (RO 16). *P. juliflora* roots are naturally abundant in Southern India, but its applicability is extremely limited. The functional groups will increase the hydrochar's absorption ability. One of the most used textile dyes is reactive dye. Covalent bonds between the dye and fabric, which have a high binding affinity for cellulose or fabric surface charges, produced this binding (Kumar *et al*., 2019). Aromatic reactive dyes are notoriously difficult to remove (Carneiro *et al*., 2005; Zhang *et al*., 2017). Hydrochar from *P. juliflora* roots was used for the first time to remove RO 16. Hydrochar dosage, solute pH, starting RO 16 concentration, and batch process temperature were optimized in this work. The aim of the study is to compare the experimental data with mathematical modeling to find out the fitting. This study has been carried out in the Environmental Engineering Laboratory of the Department of Civil Engineering, SRM Institute of Science and Technology, Kattankulathur, Chengalpattu, Tamil Nadu, India in 2022.

MATERIALS AND METHODS

P. juliflora roots were collected from Ramanad District, Southern Tamil Nadu, India. The harvested *P. juliflora* roots were allowed to naturally dry for seven days before being shredded to particle size 7.5 mm. Biomass moisture content was lowered by drying for 24 h at 103°C in an oven with hot air. In addition, this thermal biomass was destroyed at 300°C for 15 min without oxygen in an autoclave in a muffle furnace (heating rate: 5°C per minute). As soon as it reaches room temperature, the so-called hydrochar residue of this biomass was employed for adsorption investigations. In our study, hydrochar was utilized in its unmodified state (Chai *et al*., 2021). Sigma-Aldrich, India, supplied all of the compounds employed in the current experiment, including RO 16.

$C_{20}H_{17}N_3Na_2O_{11}S_3$ was the empirical formula, 617.54 g/mol was the molecular weight, and 388 nm was the wavelength of RO 16 (Kaminski *et al*., 2015).

Batch study

The batch adsorption process was run for 6 h in 250 mL conical flask with a 100-mL toiling volume using an orbital shaker. For a thorough fusing of the sorbent and dye molecules, the orbital shaker was run at 180 rpm. Following the batch trials, 5 cc of the sample was centrifuged at 1800 rpm for 5 min. Lastly, an ultra violet visible spectrophotometer was utilized to determine the sample's ultimate concentration. Eqs. 1 and 2 are used to calculate the removal efficiency in the dye (Lenin *et al*., 2021).

$$\text{Removal efficiency} = \frac{(C_0 - C_e)}{C_0} \times 100 \quad (1)$$

$$\text{Total dye removal}(\%) = \frac{m_{\text{adsor}}}{m_{\text{total}}} \times 100 \quad (2)$$

Where;

V: dye treatment volume (L)

Co: pre-adsorption concentration (mg/L)

Ce: adsorption concentration (mg/L)

Design of experiments

RSM

Minitab was used to implement Box–Behnken experimental design in response surface approach. The batch process input parameters were temperature, pH hydrochar dose, and initial RO 16 concentration. Table 1 presents a summary of the variable's many levels. Eq. 4 illustrates the RSM-developed quadratic model (Lenin *et al*., 2021).

$$Y = \beta_0 + \sum_{i=1}^{k}\beta_i x_i + \sum_{i=1}^{K}\beta_{ii} x_i^2 + \sum_{i=1}^{}0\sum_{j=i+1}\left(\beta_{ij} x_i x_{ij} + \dot{o}\right) \quad (4)$$

Where;

Y: Response (% removal efficiency),

β0, βi, βii, and βij: intercept, quadratic, linear and interaction effects

xi, xj: independent variables

ε: error.

ANFIS

ANFIS is regarded as one of the most guaranteed technologies for predicting nonlinear complex systems (Del Cerro *et al*., 2021). The present study validated ANFIS using RSM's projected experimental run. In batch experiments, a total of 31 experimental trials were used to predict clearance efficiency. The predictive model is built on the first-order Sugeno, and the resulting model for batch processes is shown in Fig. 1. ANFIS contains five layers: one input, one output, and three layers (fuzzification, logical rule, and defuzzification). Hydrochar dose, initial RO 16 concentration, pH, and temperature are the batch process inputs. The output layer for batch operations consists of a single output termed removal efficiency,

Table 1: Coded variables

Term	Coef.	SE Coef.	t-value	p-value	VIF
Constant	67.89	6.77	10.02	0.000	-
Dosage	4.05	3.66	1.11	0.285	1.00
pH	−1.58	3.66	−0.43	0.671	1.00
Initial concentration	−3.72	3.66	−1.02	0.325	1.00
Temperature	−3.72	3.66	−1.02	0.325	1.00
Dosage*dosage	0.66	3.35	0.20	0.846	1.03
pH*pH	2.06	3.35	0.61	0.548	1.03
Initial concentration*initial concentration	2.85	3.35	0.85	0.407	1.03
Temperature*temperature	2.64	3.35	0.79	0.443	1.03
Dosage*pH	2.02	4.48	0.45	0.658	1.00
Dosage*initial concentration	0.66	4.48	0.15	0.885	1.00
Dosage*temperature	−2.02	4.48	−0.45	0.658	1.00
pH*initial concentration	2.02	4.48	0.45	0.658	1.00
pH*temperature	−0.66	4.48	−0.15	0.885	1.00
Initial concentration*temperature	−2.02	4.48	−0.45	0.658	1.00

(*VIF – Variance inflation factor)

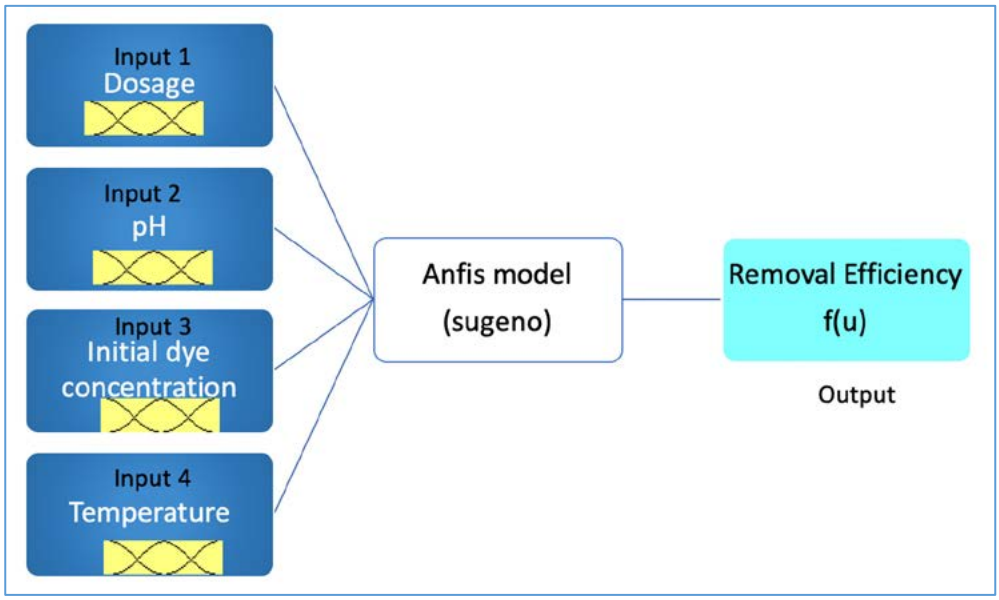

Fig. 1: ANFIS model for batch study

output membership function is the sum total of all incoming signals. Removal efficiency will result from combining these signals. The three hidden layers are membership function, logical rule, and output membership function for output prediction (Zaghloul *et al*., 2020).

Statistical error analysis

Analysis done using Eqs. 5–10 to find the model that closely resembled the experimental data (HYBRID) (Lenin *et al*., 2021).

$$\mathrm{HYBRID}(\%)=\frac{1}{N-P}\sum\left[\frac{\left(Q_{\mathrm{exp},i}-Q_{\mathrm{cal},i}\right)^2}{Q_{\mathrm{cal},i}}\right]\times 100 \quad (5)$$

Average relative error (ARE)

$$\mathrm{ARE}(\%)=\frac{100}{N}\sum_{i=1}^{N}\left[\frac{\left|Q_{\mathrm{exp},i}-Q_{\mathrm{cal},i}\right|}{Q_{\mathrm{exp},i}}\right] \quad (6)$$

Marquardt's percent standard error deviation (MPSED)

$$\mathrm{MPSED}(\%)=\sqrt{\frac{\sum\left(\frac{Q_{\mathrm{exp},}-Q_{\mathrm{cal},}}{Q_{\mathrm{exp},i}}\right)^2}{N-P}}\times 100 \quad (7)$$

Absolute average relative error (AARE) (Zaghloul *et al*., 2020)

$$\mathrm{AARE}=\frac{1}{N}\sum_{i=1}^{N}\left(\left|\frac{Q_{\mathrm{exp},i}-Q_{\mathrm{cal},i}}{Q_{\mathrm{exp},i}}\right|\right) \quad (8)$$

Adjusted R^2

$$\mathrm{Adj}R^2=1-\left[\left(1-R^2\right)*\frac{(N-1)}{(N-P-2)}\right] \quad (9)$$

Root mean square error (RMSE)

$$\mathrm{RMSE}=\sqrt{\frac{1}{N}\sum_{i=1}^{N}\left(\frac{Q_{\mathrm{exp},i}Q_{\mathrm{cal},i}}{Q_{\mathrm{exp},i}}\right)^2} \quad (10)$$

Where,

N:number of experiments,

P: factors.

Qexp,i: obtained values

Qcal,i: Model predictions.

RESULTS AND DISCUSSION

RSM for batch study

The RSM model examined linear, quadratic, and two-way variable interactions using a Box–Behnken

experimental design. The accuracy of the created model using experimental data was projected using the correlation coefficient with the highest value and the error with the lowest value. A correlation coefficient (R^2) of 0.9978 was attained with little error. This points to the fact that the derived model was highly connected with experimental data (Jaafaria *et al*., 2019). In addition, the adjusted R^2 was determined to be 0.9974, and the difference between R^2 and adj R^2 was calculated to be 0.0007, confirming adj R^2 was identical to R^2 and emphasizing the model's high significance. The adjusted R^2 was employed in the model to calculate the variance of the mean. The small difference between R^2 and adj R^2 suggests that the model's mean value is correct and that no mistake was concomitant with model terms, experimental data, or predicted data (Taran and Aghaie, 2015). The quadratic equation produced by the RSM model for calculating removal efficiency (%) is shown in Eq. 11.

$$\text{Removal efficiency} = 96.1 + 0.4(A) - 5.50(B) - 0.215(C) - 0.114(D) + 0.42(A^2) + 0.330(B^2) + 0.000730(C^2) + 0.00188(D^2) + 0.65(A*B) + 0.0084(A*C) - 0.0432(A*D) + 0.0129(B*C) - 0.0070(B*D) - 0.00086(C*D) \quad (11)$$

*A – Dosage, B – pH, C – Initial concentration, D – Temperature

The linear, quadratic, and two-way interaction models' analysis of variance is shown in Table 2. At 95% confidence, P values >0.05 are insignificant (Sodeifian *et al*., 2015). Fisher's F-value calculates the mean square error sum/residual error ratio to assess model and input parameter relevance. More relevant models have higher F-values (Yan *et al*., 2014). The model's F and P values were 372 and 0.000001, respectively, suggesting its importance. The model also showed that linear and quadratic components were significant, but two-way interactions were not (Kamyab *et al.,* 2022).

Diagnostic plots for batch study

Pareto charts and residual analysis were used to evaluate the model's relevance, which was calculated via the Pareto chart. The model produced a 2.18 t-value with 14° of freedom and 95% confidence (=0.05). Significant factors have t values >2.18. Table 2 shows that quadratic and two-way interactions are weak because linear component D (temperature) has minimal effect. Hydrochar dosage, pH, and starting RO 16 concentration affect linear and quadratic models. The Pareto analysis showed hydrochar dose and solute pH significantly affected RO 16 removal efficiency. Hydrochar dosage and solute pH exhibited the highest t-test values, 52.53 and 31.92, respectively. Fig. 3 shows

Table 2: Analysis of variance (ANOVA) for batch adsorption process

Source	DF	Adj SS	Adj MS	f-value	p-value	Remarks
Model	14	1851.11	132.222	0.41	0.000	Significant
Linear	4	1116.63	279.159	0.87	0.000	Significant
Dosage	1	392.87	392.871	1.22	0.000	Significant
pH	1	60.25	60.246	0.19	0.000	Significant
Initial concentration	1	331.82	331.824	1.03	0.000	Significant
Temperature	1	331.69	331.694	1.03	0.000	Significant
Square	4	458.67	114.668	0.36	0.835	
Dosage*dosage	1	12.47	12.469	0.04	0.000	Significant
pH*pH	1	121.30	121.297	0.38	0.000	Significant
Initial concentration*initial Concentration	1	232.60	232.605	0.72	0.000	Significant
Temperature*Temperature	1	198.93	198.928	0.62	0.000	Significant
2-Way Interaction	6	275.80	45.967	0.14	0.988	
Dosage*pH	1	65.51	65.509	0.20	0.658	
Dosage*initial concentration	1	6.88	6.884	0.02	0.885	
Dosage*temperature	1	65.51	65.509	0.20	0.658	
pH*initial concentration	1	65.51	65.509	0.20	0.658	
pH*temperature	1	6.88	6.884	0.02	0.885	
Initial concentration*temperature	1	65.51	65.509	0.20	0.658	
Error	16	0.16	0.138			
Lack-of-Fit	10	0.16	0.16	*	*	Significant
Pure error	6	0.000	0.000			
Total	30	6991.67				

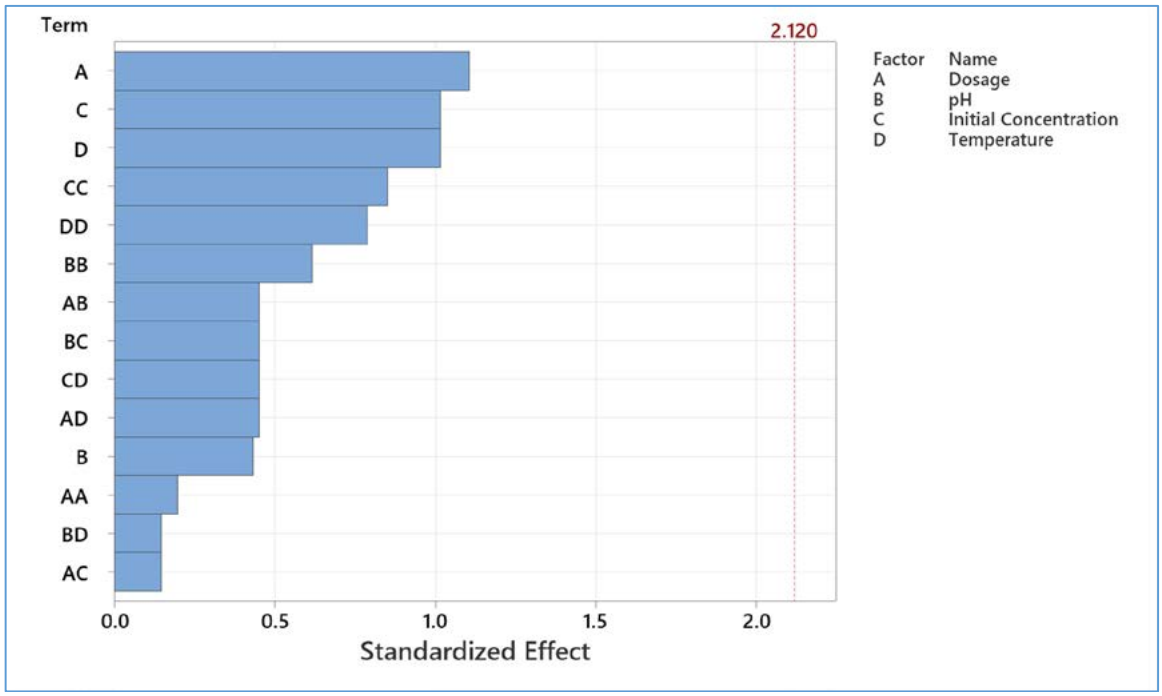

Fig. 2: Pareto chart analysis for removal efficiency

projected and actual residual error and probability graphs. Predicted values matched experimental values with a little residual error (Ahmad *et al*., 2009).

Hydrochar dosage and solute pH also affected RO 16 removal efficiency, according to the Pareto analysis in Fig. 2. The maximal t-test values for hydrochar dosage and solute pH were 52.53 and 31.92, respectively. Fig. 3 shows predicted and actual residual error and probability graphs. Predicted values matched experimental values with a minor residual error. Interpretations had a residual error ranging from +0.7 to −0.7, with observation 8 exhibiting the largest residual error of 0.7 (Xin hui *et al*., 2012).

Individual effects and interaction plots for batch study

Fig. 4 displays the effect of the influencing variables and interaction graphs. Removal effectiveness rose with an increase in hydrochar dosage, dropped with a rise in pH, declined with an increase in starting RO 16 concentration, decreased when the temperature was raised, and increased when the temperature was raised to 40°C, as shown in Fig. 4. As temperature rises, the sorbent may develop driving forces, speeding dye molecules toward it and boosting sorption. When pH rose from 2 to 4, the mean value dropped from 82.81% to 71.49%. This would be performed at a higher pH by connecting positively charged protonated hydrogen ions to the surface of the hydrochar, attracting negatively charged reactive dyes (Munagapati *et al*., 2017). Fig. 5 shows the interaction plots for removal efficiency .The removal efficacy improved as the hydrochar dosage increased, perhaps due to the existence of more binding sites at higher concentrations, resulting in enhanced adsorption capacity. The limited surface area is insufficient to absorb all of the dye molecules at a lower dosage (Aksu and Zümriye, 2005). Figs. 5 and 6 show the interactions between factors at different levels, as well as a matrix plot for a batch study.

Response optimizer for batch study

Fig. 6 shows the response optimizer improving removal efficacy. With an optimizer accuracy of 1, removal efficacy went from 86.1% to 88.12%. Ideal conditions were 2.6 g/L hydrochar, solute pH of 2, 250 mg/L RO 16, and a temperature of 38°C. Three sets of batch experiments were done under ideal settings to measure removal efficacy, and the results indicated an average removal rate of 87.92%.

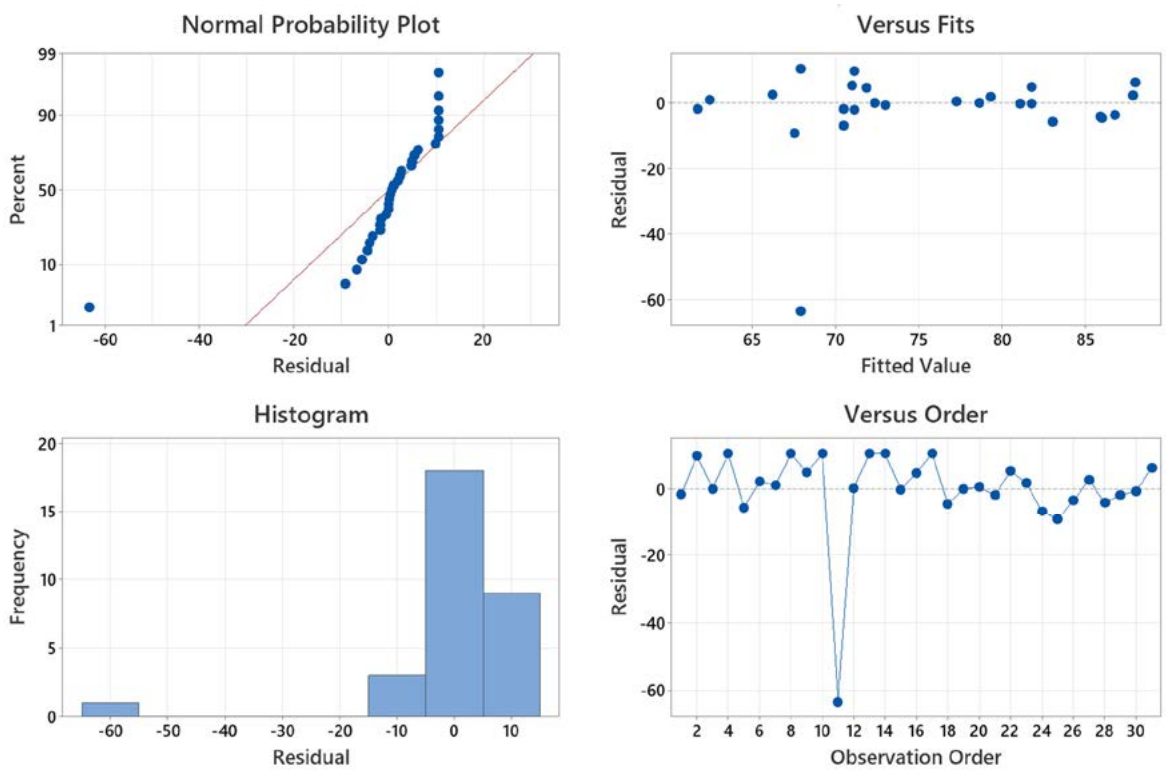

Fig. 3: Residual plots for removal efficiency

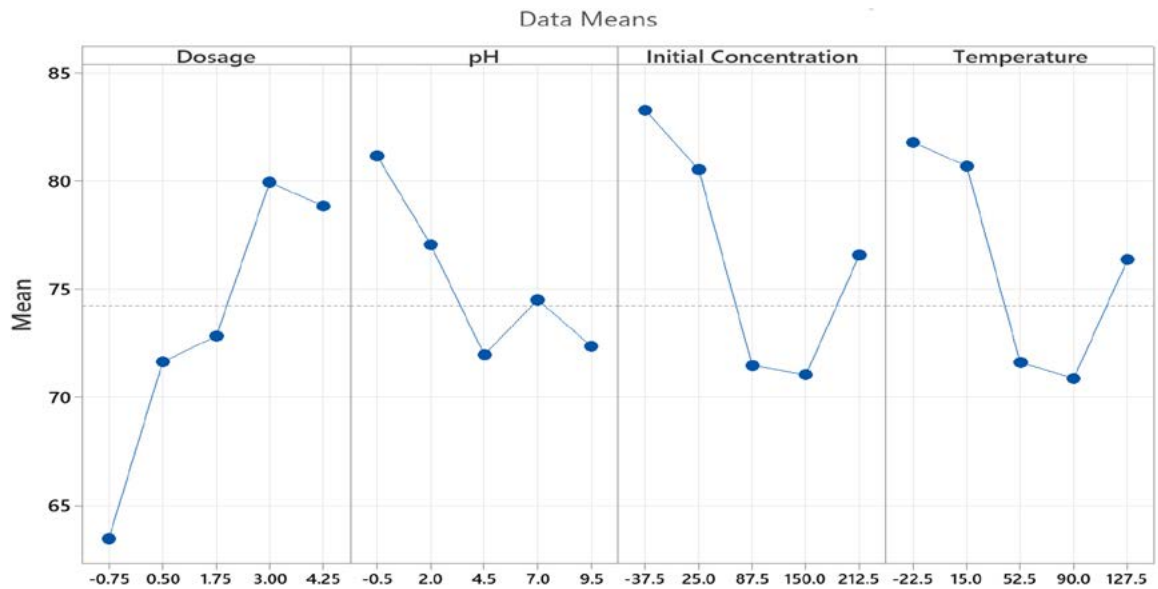

Fig. 4: Main effect plots

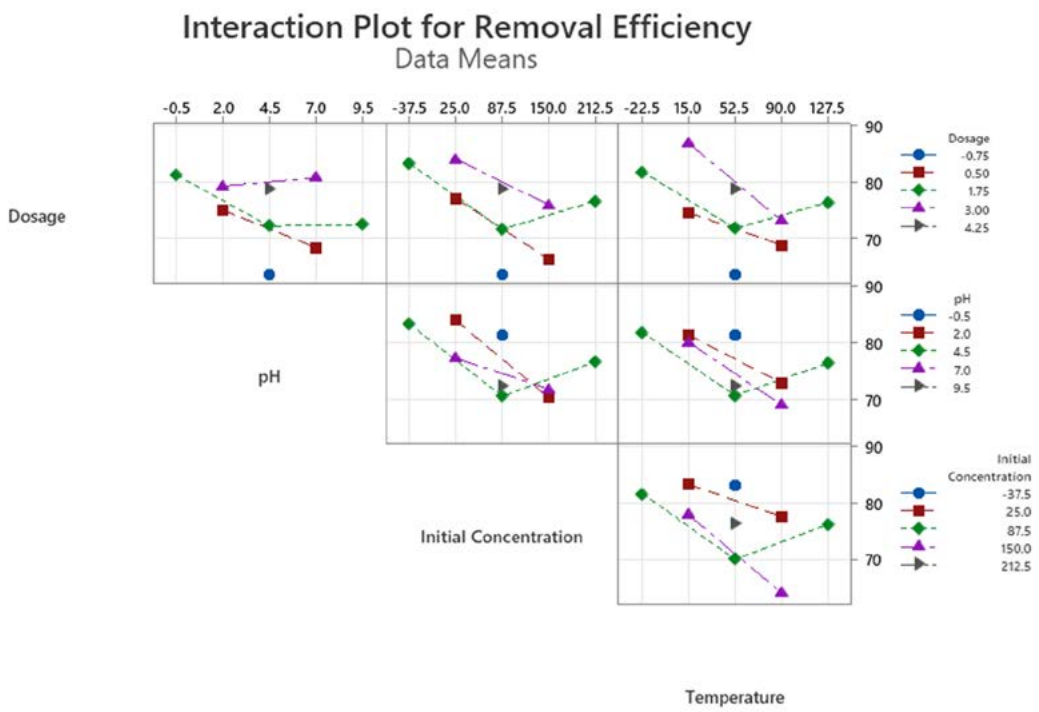

Fig. 5: Interaction plots for removal efficiency

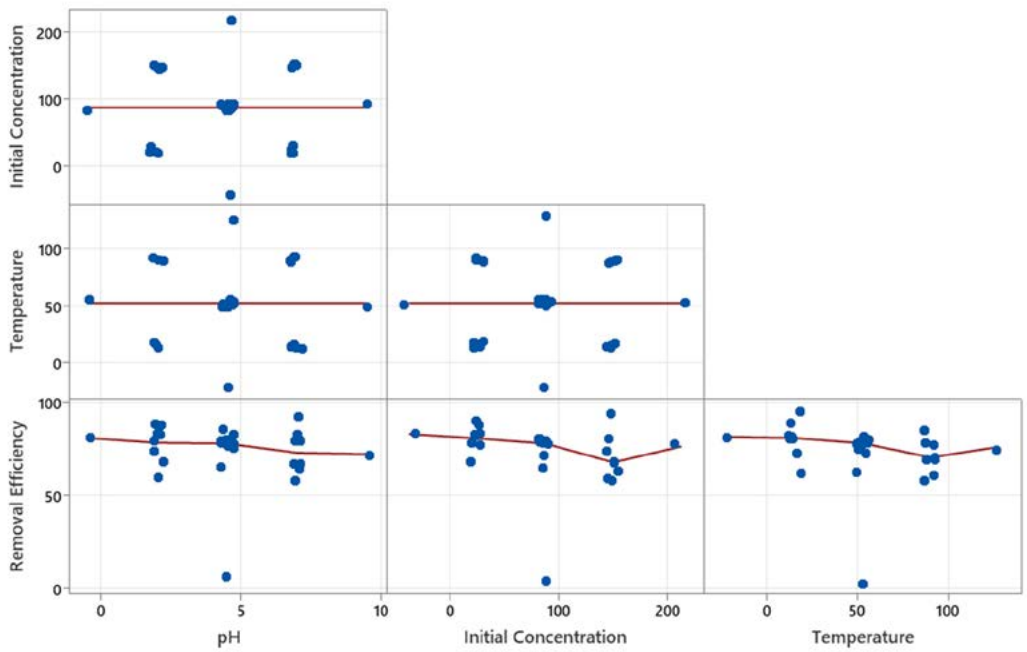

Fig. 6: Matrix plot

ANFIS for batch study

Experimental data were evaluated using a hybrid least square and gradient technique. Fig. 7 shows a grid partitioned Sugeno-type structural model for removal efficacy assessment. Four input variables were utilized to produce a single output, with low, medium, and high membership functions applied to each. With minor errors, a correlation coefficient of 0.9999 between the experimental and projected values reveals that the model best matches the experimental data. ANFIS trains data using fuzzy inference with multiple hidden neural networks, which reduces errors and improves model accuracy. Epoch 3 has a 0.000075 mean square error. This points toward the model's accuracy in predicting RO 16 elimination efficiency. Table 3 contains a detailed description of the expected removal efficiency for each trial (Ghorbani *et al*., 2016). A surface map was also constructed to better understand the interaction between the input variables, as seen in Fig. 8. As shown in Fig. 8, removal efficiency improved when the hydrochar dosage was increased, the pH was dropped, the starting RO 16 concentration was decreased, and the temperature was reduced from 30°C to 35°C, with a further temperature rise to 40°C, boosting removal efficacy. Fig. 8a, for example, demonstrates the relationship between hydrochar dosage (A) and pH (B) in terms of removal efficiency. The removal effectiveness improved as the hydrochar dosage increased from 1 to 3 g/L, but decreased when the pH increased from 2 to 4. The highest removal effectiveness of 85.6% was observed with a hydrochar dosage of 3 g/L and pH 2.

Statistical and residual errors assessed experimental, RSM, and ANFIS correctness. Table 3 demonstrates experimental, RSM, and ANFIS elimination effectiveness at different levels of residual errors for each model. At pH 2, 2 g/L hydrochar, 500 mg/L RO 16, and 35°C, 86.1% removal was achieved. Under identical process settings, RSM and ANFIS removed 86.3% and 86.1%, respectively. The findings show that RSM and ANFIS projected values match real data, and the residual error between experimental and model data is minimized. RSM correlated 0.978 and ANFIS 0.9999. ANFIS data matched experimental data better than RSM, with reduced residual error. The RSM correlation coefficient was 0.978 (Zaghloul *et al*., 2020).

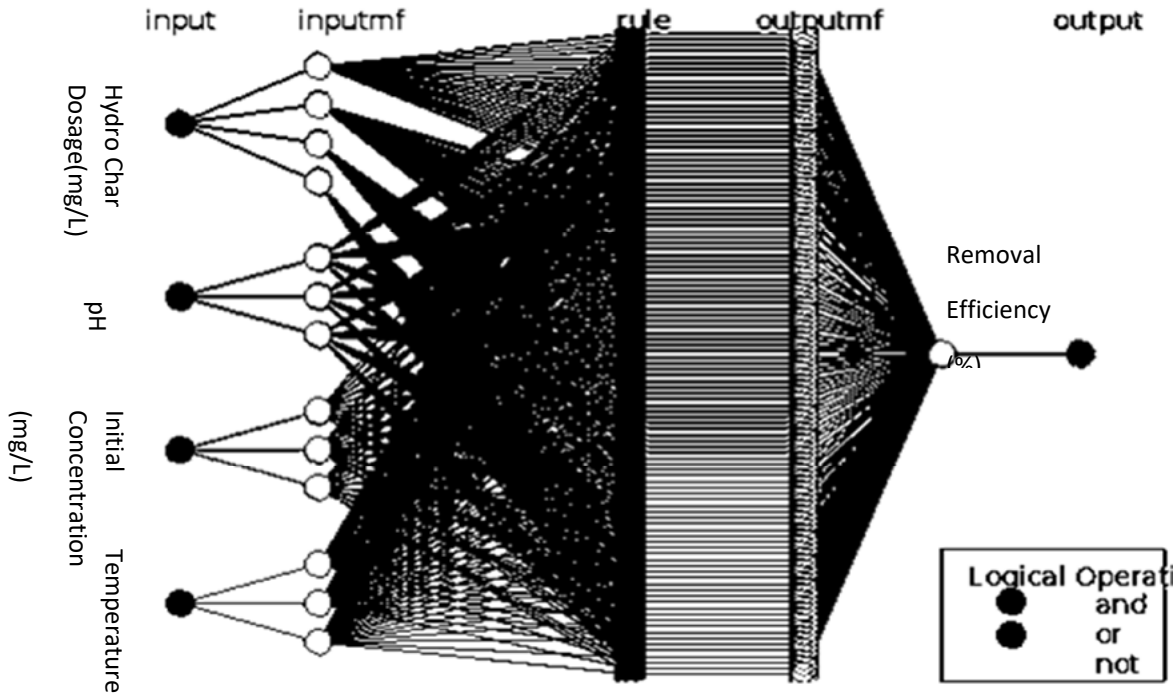

Fig. 7: ANFIS for batch study

Table 3: Removal efficiency of experimental, RSM and ANFIS models for batch study

Dosage	pH	Initial concentration	Temperature	Removal efficiency	RSM	ANFIS
0.5	7	150	90	60.065	60.2	60.1
0.5	7	25	15	81.0075	81.3	81.2
0.5	2	150	15	72.415	72.7	72.6
1.75	4.5	87.5	52.5	78.45875	78.8	78.8
0.5	2	25	90	77.4575	77.5	77.3
3	2	25	15	90.1975	90.4	90.6
0.75	4.5	87.5	52.5	63.49	63.8	63.5
1.75	4.5	87.5	52.5	78.45875	78.7	78.9
3	2	25	90	86.6475	86.8	86.3
1.75	4.5	87.5	52.5	78.45875	78.9	78.8
1.75	4.5	87.5	52.5	4.5	4.6	4.7
4.25	4.5	87.5	52.5	78.83375	78.9	78.8
1.75	4.5	87.5	52.5	78.45875	78.6	78.4
1.75	4.5	87.5	52.5	78.45	78.7	78.5
3	2	150	15	81.605	81.8	81.6
1.75	4.5	212.5	52.5	76.58	76.7	76.6
1.75	4.5	87.5	52.5	78.45875	78.6	78.7
3	7	25	15	81.3975	81.5	81.4
0.5	2	25	15	81.0075	81.1	81.4
3	7	25	90	77.8475	77.9	77.7
0.5	7	25	90	68.6575	68.7	68.8
1.75	4.5	87.5	52.5	76.35875	76.5	76.4
1.75	0.5	87.5	52.5	81.15875	81.4	81.3
0.5	7	150	15	63.615	63.7	63.5
3	2	150	90	58.315	58.4	58.7
1.75	4.5	-37.5	52.5	83.2775	83.3	83.4
0.5	2	150	90	68.865	68.9	68.9
1.75	4.5	87.5	22.5	81.7825	81.8	81.9
3	7	150	90	69.255	69.4	69.3
1.75	9.5	87.5	52.5	72.35875	72.5	72.4
3	7	150	15	94.24	94.6	94.6

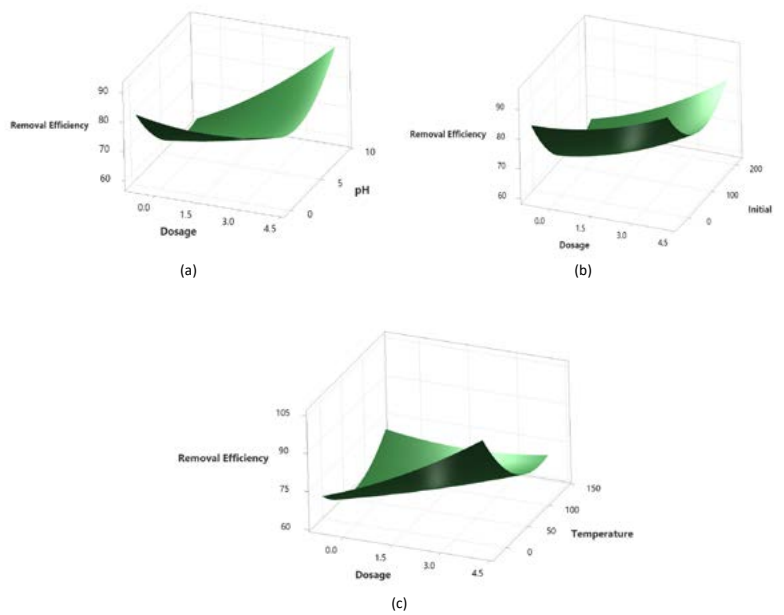

Fig. 8: (a) Surface plot of removal efficiency vs, pH, dosage,(b) Surface plot of removal efficiency vs. initial concentration, dosage (c) Surface plot of removal efficiency vs. temperature, dosage

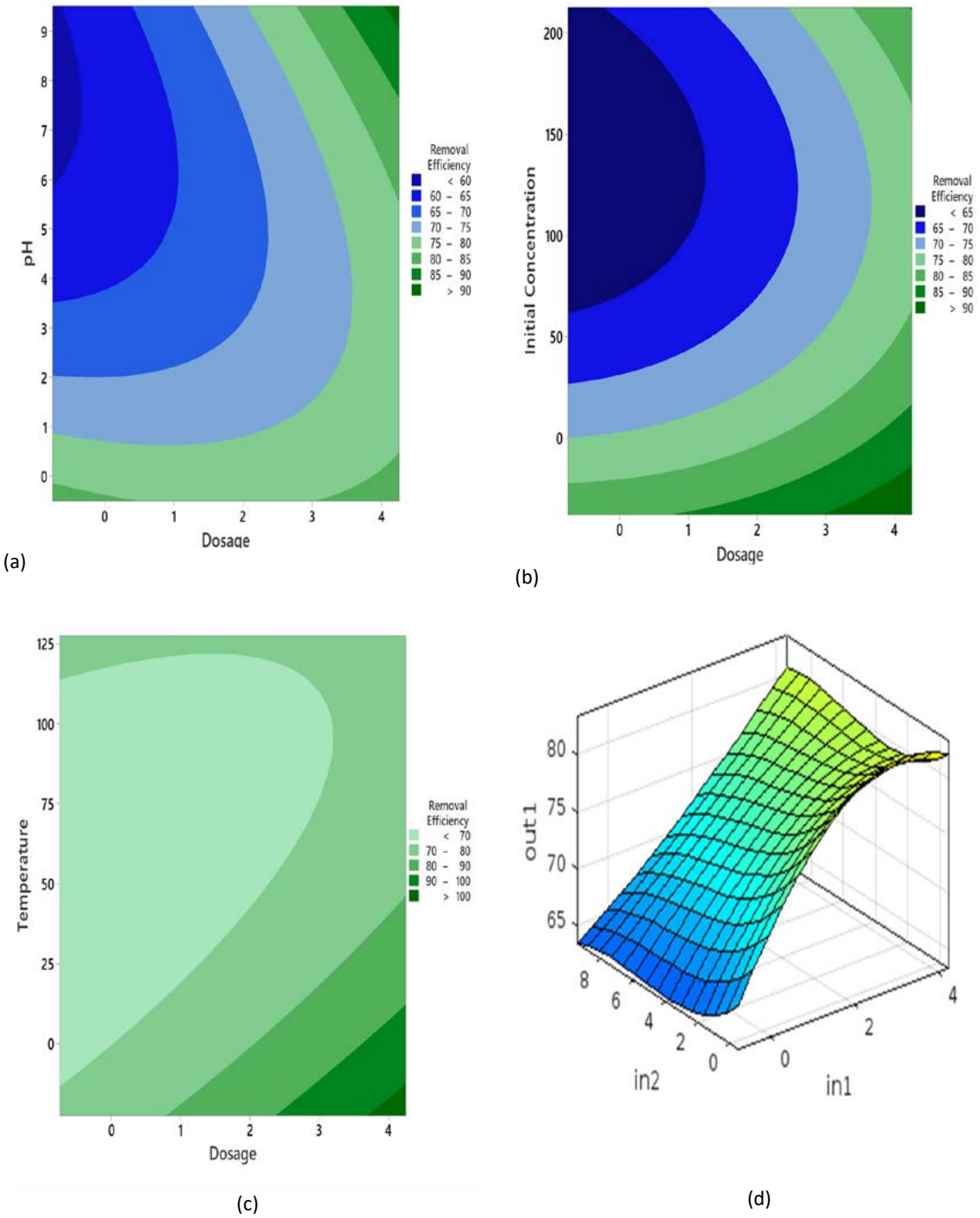

Fig. 9: (a) Contour plot of removal efficiency vs pH, dosage (b) Contour plot of removal efficiency vs initial concentration, dosage (c) Contour plot of removal efficiency vs. temperature, dosage (d) ANFIS surface plot for batch study

Fig. 10:

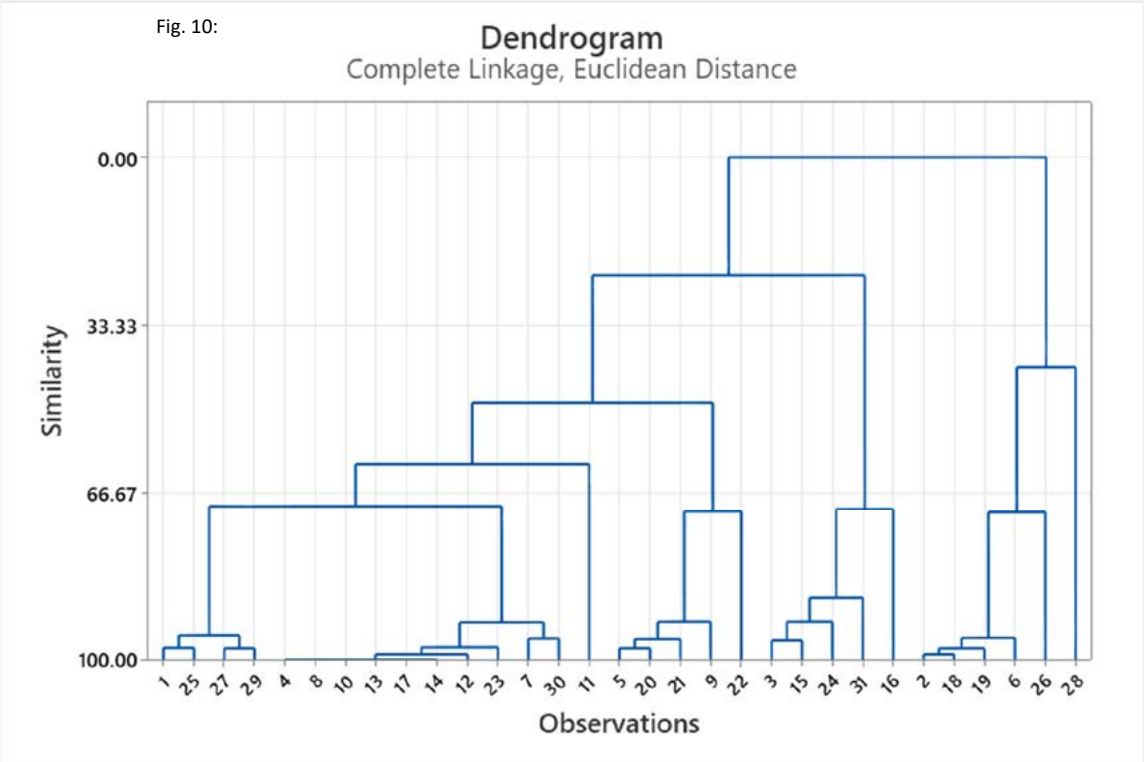

Fig. 10: Cluster analysis

Table 4: Statistical error analysis

S.No	Error function	RSM	ANFIS
1	AARE	0.00003	0.00002
2	HYBRID	0.0015	0.00019
3	ARE	0.00125	0.00048
4	MPSED	0.00758	0.00285
5	RMSE	0.00009	0.00005
6	Adj R^2	0.9981	0.9999
7	R^2	0.9988	0.9999

Dosage Variable cluster analysis compares experimental variables with RSM and ANFIS in Fig. 10. It shows an experimental and RSM cluster with 99.99 similarity and zero distance. Experimental and RSM data created the second cluster with a similarity of 99.94 and a distance of 0.001. Experimental data matched ANFIS results.

Statistical Error analysis verified the model's accuracy and precision against experimental data. Table 4 shows experimental, RSM, and ANFIS model statistical errors. It shows that both models had insignificant errors, and the RSM and ANFIS correlation coefficients were 0.9988 and 0.9999, respectively. The present correlation coefficient is extremely high and confirms the model's fit, according to Joglekar and May (Lenin *et al*., 2021). To determine if RSM and ANFIS were overpredicted, the corrected R^2 was 0.9988 and 0.9999, respectively. These findings demonstrated that the model's predicted values match the experimental data. The fact that the ANFIS model outperformed the RSM model was proved by the fact that the ANFIS model had a higher correlation coefficient and fewer mistakes. adj R^2 was 0.9981 and 0.9999. The model's ANOVA shows that the difference between R^2 and adj R^2 was 0.0011 and <0.1, proving its

Table 5: Overview of work carried out using RSM

Anaerobic reactor	Type of pollutant	Method	Runs	Dependant variables	Independent variables
Batch reactor (Kainthola *et al*., 2018)	Rice straw hydrilla verticillata	CCD	20	C/N ratio, F/M ratio, pH	methane yield
Hybrid bioreactor (Mortezaei *et al*., 2018)	Yogurt effluent	CCD	19	COD influent	HRT
Batch reactor (Safari *et al*., 2018)	Cattle manure and canola residues	Box–Behnken	29	Temperature	Stirring time
MASBR (Rajasimman *et al*., 2017)	Textile waste water	CCD	13	Sorbent dosage	Biomass support
Batch reactor (Jacob S *et al*., 2016)	Potato waste and aquatic weed	CCD	20	Total solid, Proportion of co-support, Inoculum concentration	Methane yield
Floating drum anaerobic digester (Sathish and Vivekanandan *et al*., 2016)	Rice straw	CCD	30	Temperature, pH, Substrate concentration	Biogas yield
Mixed plug-flow reactor (Rasouli *et al*., 2015)	Cow manure	CCD	18	OLR, Temperature, Mixing level	Biogas Production, Methane yield
Batch reactor (Sajeena *et al*., 2014)	Organic fraction municipal solid waste	CCD	20	pH, Substrate concentration, TOC	Biogas production
Batch and Column reactor (Lenin *et al*.,2021)	Reactive Red 120 dye	Box–Behnken	27	Dosage, pH, Concentration, Temperature,bed depth,flow rate	Removal Efficiency
This study	Reactive orange 16 dye	Box Behnken	31	Dosage, pH, Concentration, Temperature	Removal Efficiency

capacity to predict words. It shows that all linear and quadratic components are significant, and the two-way interaction is inconsequential, making the model significant. The Fisher F test scored 63.24, suggesting that the model matches the experimental data.

Table 5 summarizes RSM predicted work compared with that of this present study with the type of pollutant used, method, number of runs, dependent variables, and independent variables.The initial RSM design technique—CCD, BBD, or FFD—received the greatest attention from researchers. Most reactors investigated four or fewer parameters, and the most common were methane output, biogas generation rate,and COD removal efficiency. To better understand their applications, such as the BBD method used in trials with various parameters, techniques other than CCD must be optimized and designed. RSM may model and optimize more than four effective factors to boost meaningfulness and comprehensiveness (Jasni *et al*., 2020).

CONCLUSIONS

RSM uses predictor variables and dependent variables or responses. It is more practical than statistical significance tests for optimizing variables/ factors (point estimate is the statistical jargon). Two case studies showed that the ANFIS was faster and more accurate than standard optimization approaches such as the genetic algorithm. The ANFIS produced all fuzzy inference system-required fuzzy data. Fuzzy inference system reduces application development, execution, and maintenance expenses, among others. Fuzzy inference systems are more compact (require fewer rules); encode high-level information even in the designer's native language; are less error-prone; can handle ambiguous, uncertain, and imprecise input; are simpler to maintain. Finally, Sugeno FIS can model and create hybrid systems such as ANFIS and linguistic hedges. RO 16 was batch sorptioned on *P. juliflora root* hydrochar in this study, and RSM and ANFIS optimized process conditions.

At pH 2, 2 g/L hydrochar dosage, 35°C temperature, and 250 mg/L starting RO 16 concentration, removal effectiveness reached 86.1%. ANFIS predicted higher values than RSM, with batch correlation coefficients of 0.9999 and 0.9997, respectively. Four input variables were utilized to produce a single output, with low, medium, and high membership functions applied to each. With minor errors, a correlation coefficient of 0.9999 between the experimental and projected values reveals that the model best matches the experimental data.This study shows that mathematical techniques can accurately estimate dye removal efficiency from aqueous solutions.

AUTHOR CONTRIBUTIONS

K. Prasanna reviewed the literature and evaluated the results, whereas J. Oliver Paul Nayagam conducted the experiments, analysed and wrote the report.

ACKNOWLEDGEMENT

Authors are grateful to SRMIST management and the Head of Department of Civil Engineering for supporting this extensive research.The SRMIST Environmental Engineering Lab supported the experimental investigation. Authors thank the Material Characterization Facility (Department of Physics and Nanotechnology) and School of Bioengineering.

CONFLICT OF INTEREST

The author declares that there is no conflict of interests regarding the publication of this manuscript. In addition, the ethical issues, including plagiarism, informed consent, misconduct, data fabrication and/or falsification, double publication and/or submission, and redundancy have been completely observed by the authors.

OPEN ACCESS

PUBLISHER'S NOTE

ABBREVIATIONS

°C	Degree Celcius
AARE	Absolute average relative error
Adj MS	Adjusted mean squares
Adj SS	Adjusted sums of squares
ANFIS	Adaptive Neuro-Fuzzy Inference System
ANOVA	Analysis of variance
$C_{20}H_{17}N_3Na_2O_{11}S_3$	Emprical formula for Reactive Orange 16
cc	cubic centimeters
CC	Cubic Capacity
Ce	concentration after adsorption
CI	confidence interval
Co	concentration before adsorption
DF	Degrees of freedom
e.g	Exempli gratia (for example)
f-value	ratio of two variances
g/L	gram/litre
g/mol	Gram per molecule
Hz	Hertz
i.e.	Id est (that is)
kg	Kilogram
km	Kilometer
m	Meter
M	Magnitude
m/s	Meter per second (velocity unit)
m^2	Meter square
MASW	Pearson correlation coefficient
mg/L	Milli gram per litre
MPSED	Marquardt's percent standard error deviation
N	number of experimental observations

nm	Nano metre
NN	Neural Network
P	Number of factors
p-value	probability value
PI	Profitability Index
Qcal,i	calculated or predicted values of the models
Qexp,i	xperimental values
RMSE	Root mean square error
RO 16	Reactive Orange 16
rpm	Revlotions per minute
RSM	Response Surface Methodology
SE	standard error
T test	statistical test that is used to compare the means of two groups
V	total volume of dye to be treated
xi, xj	Independent variables
Y	Response
β0	Intercept
βi	quadratic
βii	linear
βij	Interaction effects
ε	Error

REFERENCES

Ahmad A.A.; Hameed, B.H.; Ahmad, A.L., (2009). Removal of disperse dye from aqueous solution using waste derived activated carbon: Optimization study. J. Hazard. Mater., 170 (2–3): 612–619 **(8 pages).**

Aksu, Z., (2005). Application of biosorption for the removal of organic pollutants: A review. Process Biochem., 40(3–4): 997–1026 **(30 pages).**

Aravind, J.; Kanmani, P.;Sudha, G.; Balan, R., (2016). Optimization of chromium(VI) biosorption using gooseberry seeds by response surface methodology. Global J. Environ. Sci. Manage., 2(1): 61-68 **(8 pages).**

Beesley, L.; Moreno, J.E.; Gomez, J.L.; Harris, E.; Robinson, B.; Sizmur, T., (2011). A review of biochars potential role in the remediation; revegetation and restoration of contaminated soils. Environ. Pollut., 159(12): 3269–3282 **(14 pages).**

Carneiro, P.A.; Osugi, M.E.; Fugivara, C.S.; Boralle, N.; Furlan, M; Valnice, M.; Zanoni, B., (2005). Evaluation of different electrochemical methods on the oxidation and degradation of reactive blue 4 in aqueous solution. Chemosphere. 59(3): 431–439 **(9 pages).**

Chai, W.S.; Cheun, J.Y.; Kumar, P.S.; Mubashir, M.; Majeed, Z.; Banat, F.; Ho, S.H.; Show, P.L., (2021). A review on conventional and novel materials towards heavy metal adsorption in wastewater treatment application. J. Clean. Prod., 296: 1–15 **(15 pages).**

Chinwetkitvanich, S.; Tuntoolvest, M; Panswad, T., (2000). Anaerobic decolorization of reactive dyebath effluents by a two-stage UASB system with tapioca as a co-substrate. Water Res., 34(8): 2223–2232 **(10 pages)**.

Crini, G., (2006). Non-conventional low-cost adsorbents for dye removal: a review. Bioresour. Technol., 97(9): 1061–1085 **(25 pages)**.

Deb, A.; Debnath, A.; Saha, B., (2020). Ultrasound aided rapid and enhanced adsorption of anionic dyes from binary dye matrix onto novel hematite/polyaniline nanocomposite: Response surface methodology optimization. Appl. Organomet. Chem., 34(2): 1–20 **(20 pages)**.

Del Cerro, R.T.G.; Subathra, M.S.P.; Kumar, N.M.; Verrastro, S.; George, S.T., (2021). Modelling the daily reference evapotranspiration in semi-arid region of South India: A case study comparing ANFIS and empirical models. Inf. Process. Agric., 8(1): 173–184 **(12 pages)**.

Ghoneim, M.M.; El-Desoky, H.S.; El-Moselhy, K.M.; Amer, A.; Abou El-Naga, E.H.; Mohamedein, L.I.; Al-Prol, A.E., (2014). Removal of cadmium from aqueous solution using marine green algae, Ulva lactuca. Egypt. J. Aquatic Res., 40(3): 235–242 **(8 pages)**.

Ghorbani, F.; Kamari, S., (2016). Application of response surface methodology for optimization of methyl orange adsorption by Fe-grafting sugar beet bagasse. Adsorpt. Sci. Technol. 35(4): 317–338 **(22 pages)**.

Gopal, N.; Asaithambi, M.; Sivakumar, P.; Sivakumar, V., (2014). Adsorption studies of a direct dye using polyaniline coated activated carbon prepared from Prosopis juliflora. J. Water Process. Eng., 2: 87–95 **(9 pages)**.

Gupta, V.K.; Kumar, R.; Nayak, A.; Saleh, T.A.; Barakat, M.A., (2013). Adsorptive removal of dyes from aqueous solution onto carbon nanotubes: a review. Adv. Colloid Interface Sci., 193: 24–34 **(11 pages)**.

Hussein, H.; Ghada, S. A.; Sami, A. S.; Rehab, M., (2018). Bioremediation of methyl orange onto nostoc carneum biomass by adsorption kinetics and isotherm studies. Res. J. Microbiol., 1: 6–22 **(17 pages)**.

Jaafaria, J.; Yaghmaeiana, K., (2019). Response surface methodological approach for optimizing heavy metal biosorption by the blue-green alga chroococcus disperses. Desalination Water Treat., 142: 225–234 **(10 pages)**.

Jacob, S.; Banerjee, R., (2016). Modeling and optimization of anaerobic codigestion of potato waste and aquatic weed by response surface methodology and artificial neural network coupled genetic algorithm, Bioresour. Technol., 214: 386–395 **(10 pages)**.

Jasni, A. B.; Kamyab, H.; Chelliapan, S.; Arumugam, N.; Krishnan, S.;Din, M. F. M., (2020). Treatment of wastewater using response surface methodology: A brief review. Chem. Eng. Trans., 78: 535–540 **(6 pages)**.

Kainthola, J.; Kalamdhad, A. S.; Goud, V. V., (2018). Optimization of methane production during anaerobic co- digestion of rice straw and hydrilla verticillata using response surface methodology. Fuel. 235: 92–99 **(8 pages)**.

Kaminski, W.; Tomczak, E.; Tosik, P., (2015). Kinetics of azo dyes sorption onto low-cost sorbents. Desalination Water Treat., 55(10): 2675–2679 **(5 pages)**.

Kamyab, H.; Yuzir, M. A.; Riyadi, F. A.; Ostadrahimi, A.; Khademi, T.; Ghfar, A. A.; Kirpichnikova, I., (2022). Electrochemical oxidation of palm oil mill effluent using platinum as anode: Optimization using response surface methodology. Environ. Res. , 214: 113993: 1–10 **(10 pages)**.

Kaur, A.; Sharma, S., (2017). Removal of heavy metals from waste water by using various adsorbents-a review. Indian J. Sci. Technol., 10(34): 1–14 **(14 pages)**.

Kumar, P.S.; Joshiba, G.J.; Femina, C.C.; Varshini, P.; Priyadharshini, S.; Karthick, M.A.; Jothirani, R., (2019). A critical review on recent developments in the low-cost adsorption of dyes from wastewater. Desalination Water Treat., 172: 395–416 **(22 pages)**.

Lenin, S.M.; Kalyani, G.; Gokulan, R.; Ragunath, S.; Joga Rao, H., (2021). Comparative adsorptive removal of reactive red 120 using RSM and ANFIS models in batch and packed bed column. Biomass Convers. Biorefin., 1–17 **(17 pages)**.

Mortezaei, Y.; Aman, T.; Elyasi, S., (2018). High-rate anaerobic digestion

of yogurt wastewater in a hybrid EGSB and fixed-bed reactor: Optimizing through response surface methodology. Process Saf. Environ. Prot.,113: 255–263 **(9 pages)**.

Munagapati, V.S.; Yarramuthi, V.; Kim, Y.; Lee, K.M.; Kim, D.S., (2018). Removal of anionic dyes (Reactive Black 5 and Congo Red) from aqueous solutions using banana peel powder as an adsorbent. Ecotoxicol. Environ. Saf., 148: 601–607 **(7 pages)**.

Nayagam, J.O.P.; Prasanna, K., (2021). Utilization of shell-based agricultural waste adsorbents for removing dyes: A review. Chemosphere. 132737: 1–17 **(17 pages)**.

Ohale, P.E.; Uzoh, C.F.; Onukwuli, O.D., (2017). Optimal factor evaluation for the dissolution of alumina from azaraegbelu clay in acid solution using RSM and ANN comparative analysis. S. Afr. J. Chem. Eng., 24(1): 43–54 **(12 pages)**.

Orshansky, F.; Narkis, N., (1997). Characteristics of organics removal by PACT simultaneous adsorption and biodegradation. Water Res., 31(3): 391–398 **(8 pages)**.

Rajasimman, M.; Babu, S. V.; Rajamohan, N., (2017). Biodegradation of textile dyeing industry wastewater using modified anaerobic sequential batch reactor start up, parameter optimization and performance analysis. J.Taiwan. Inst. Chem. Eng., 72: 171–181 **(11 pages)**.

Rasouli, M.; Ajabshirchi, Y.; Mousavi, S.M.; Nosrati, M.; Yaghmaei, S., (2015).Process optimization and modeling of anaerobic digestion of cow manure for enhanced biogas yield in a mixed plug-flow reactor using response surface methodology. Biosci. Biotechnol. Res. Asia., 12: 2333–2344 **(12 pages)**.

Safari, M.; Abdi, R.; Adl, M.; Kafashan, J., (2018). Optimization of biogas productivity in lab-scale by response surface methodology. Renew. Energy. 118: 368–375 **(8 pages)**.

Sajeena, B.B.; Jose, P.P.; Madhu, G., (2014). Optimization of process parameters affecting biogas production from organic fraction of municipal solid waste via anaerobic digestion. Int. J. Biol., 8(1): 43–48 **(6 pages)**.

Sathish, S.; Vivekanandan, S., (2016). Parametric optimization for floating drum anaerobic bio-digester using response surface methodology and artificial neural network. Alex. Eng. J., 55: 3297–3307 **(11 pages)**.

Sodeifian, G.; Sajadian, S.A.; Ardestani, N.S., (2016). Evaluation of the response surface and hybrid artificial neural network-genetic algorithm methodologies to determine extraction yield of Ferulago angulata through supercritical fluid. J. Taiwan Institute Chem. Eng., 60: 165–173 **(9 pages)**.

Taran, M.; Aghaie, E., (2015). Designing and optimization of separation process of iron impurities from kaolin by oxalic acid in bench scale stirred tank reactor. Appl. Clay Sci., 107: 109–116 **(8 pages).**

Tejada, T.C.; Villabona,O. Á.; Gonzalez Á.D., (2021). Adsorption of azo-anionic dyes in a solution using modified coconut (Cocos nucifera) mesocarp: Kinetic and equilibrium study. Water. 13(10): 1–10 **(10 pages).**

Tran, T.H.; Le, A.H.; Pham, T.H.; Nguyen, D.T.; Chang, S.W.; Chung, W.J.; Nguyen, D.D., (2020). Adsorption isotherms and kinetic modeling of methylene blue dye onto a carbonaceous hydrochar adsorbent derived from coffee husk waste. Sci.Total Environ., 725: 1–35 **(35 pages)**.

Wu, J.S.; Liu, C.H.; Chu, K.H.; Suen, S.Y., (2008). Removal of cationic dye methyl violet 2B from water by cation exchange membranes. J. Membr. Sci., 309(1-2): 239–245 **(7 pages)**.

Xin hui, D.; Srinivasakannan, C.; Qu, W.W.; Xin, W.; Jin-hui, P.;Li-bo, Z., (2012). Regeneration of microwave assisted spent activated carbon: process optimization, adsorption isotherms and kinetics. Chem. Eng. Process., 53: 53–62 **(10 pages)**.

Yan, Y.; Xiang, B.; Yi, X.; Li, Y.; Jia, Q., (2014). Competitive adsorption of acid dyes from aqueous solution on diethylenetriamine modified chitosan beads. J. Appl. Polym. Sci., 131(23): 1–9 **(9 pages)**.

Yousif, N.; Cole, J.; John, C. R.; Diedrichsen, J.; Karl, E.Z.; Carolee, J.W.; Dorsa B.K., (2018). Textile industry wastewaters treatment. J. Phys. Ther. Sci., 9(1): 1–11 **(11 pages)**.

Zaghloul, M.S.; Hamza, R.A.; Iorhemen, O.T.; Tay, J.H., (2020). Comparison of adaptive neuro-fuzzy inference systems (ANFIS) and support vector regression (SVR) for data-driven modelling of aerobic granular sludge reactors. J. Environ. Chem. Eng., 8(3): 1–20 **(20 pages).**

Zhang, Y.; Huang, G.; An, C.; Xin, X.; Liu, X.; Raman, M.; Doble, M., (2017). Transport of anionic azo dyes from aqueous solution to gemini surfactant-modified wheat bran: Synchrotron infrared, molecular interaction and adsorption studies. Sci.Total Environ., 595: 723–732 **(10 pages)**.

AUTHOR (S) BIOSKETCHES

Oliver Paul Nayagam, J., Ph.D. Candidate, Research Scholar, Department of Civil Engineering, SRM Institute of Science and Technology, Kattankulathur, Chengalpattu, Tamil Nadu, India.
- Email: *oj1145@srmist.edu.in*
- ORCID: 0000-0001-8887-1713
- Web of Science ResearcherID: HGC-7377-2022
- Scopus Author ID: 57209465270
- Homepage: https://alumni.srmist.edu.in/p/oliver-p.dz

Prasanna K., Ph.D, Assistant Professor, Department of Civil Engineering, SRM Institute of Science and Technology, Kattankulathur, Chengalpattu, Tamil Nadu, India.
- Email: *prasannk@srmist.edu.in*
- ORCID: 0000-0001-7839-4503
- Web of Science ResearcherID: ABE-6762-2021
- Scopus Author ID: 55749479300
- Homepage: https://www.srmist.edu.in/faculty/dr-k-prasanna-2/

HOW TO CITE THIS ARTICLE

Oliver Paul Nayagam, J.; Prasanna, K., (2023). Response surface methodology and adaptive neuro-fuzzy inference system for adsorption of reactive orange 16 by hydrochar. Global J. Environ. Sci. Manage, 9(3): 373-388.

DOI: 10.22035/gjesm.2023.03.03

url: https://www.gjesm.net/article_698518.html